Research paper **Open Access**

Electrochemical properties of reduced graphene oxide-polyaniline composite

E.E. El-Shereafy[1], W. A. Bayoumy[2], K. Faisal [2], M. A. Mousa[2]
[1]Chemistry Department, Faculty of Science- Menofia University, Egypt
[2]Chemistry Department, Faculty of Science- Benha University, Egypt

Abstract

Polyaniline (PANI), reduced graphene oxide (rGO), and rGO@PANI composite were prepared and characterized by X-ray diffraction (XRD), Fourier transforms infra-red (FT-IR), scan electron microscopy (SEM). The electrochemical properties were studied by using cyclic voltammetry (CV) , galvanostatic charge-discharge (GCD), and electrochemical impedance methods (EIS). The composite of PANI and G (rGO@PANI) has a specific capacitance of 22.3 F/g, an energy density of 6.5 Wh /kg, and a power density of 153 W/kg at 0.5 A/g and great cycling performance, with 81.2% capacitance retained over 250 cycles. PANI enhances the conduction of electrons and so rGO individually. The formation of the emeraldine base for PANI decreases the rate of faradaic process in the composite and leads to decrease in the total capacitance.

1. Introduction

Polyaniline (PANI) as one of conducting polymers [1,2] is broadly studied due to of its a few remarkable properties [3], like the simplicity of preparation, low cost, lightweight, optical properties, better electronic, soluble in different solvents, highly stable in air, and great processability [4-6]. Moreover, it can be utilized in many applications, such as corrosion protection coatings [7], rechargeable batteries [8], microwave absorption [9], electromagnetic interference shielding, as well as electrodes and sensors [10]. PANI displays dramatic variations in its electronic structure and physical properties at protonated state. Based on the oxidation level, PANI can be combined in many insulating forms such as the fully reduced leucoemeraldine base (LEB), half oxidized emeraldine base (PANI-EB) and completely oxidized pernigraniline base (PNB). The PANI-EB is the steadiest and broadly explored polymer in this group. PANI-EB varies openhandedly from LEB and PNB as in its conductivity can be changed by doping from 10^{-1} up to 100 S/cm and more, while LEB and PNB structure are not conducting [11]. The conducting emeraldine salt structure (PANI-ES) is accomplished by doping with aqueous acids where H^+ ions are adjoined to the –N= sites. This causes an enhancement in the conductivity of several ten orders of magnitude depending on the technique for handling [12]. According to the above mentioned properties and applications, PANI was composed with carbon-based materials like (reduced graphene oxide [12], carbon nanotube, and graphene oxide [13], different metal oxides, inorganic perovskites [14], or even with a combined system to increase its electronic behaviors [15].

Graphene is an allotrope of carbon as a two-dimensional with one atom thick, the honey-comb cross section in which one atom forms every vertex. It is considered as an essential building block for all sp^2 graphitic materials. Graphene has several unexpected properties. It conducts heat and electricity usefully and is almost transparent [16]. Scientists have distinguished the bipolar transistor and large quantum oscillations in the graphene. Currently, several methods had been investigated to prepare graphene. Few and single-layer graphene initially can be acquired by mechanical peeling ("Scotch-tape" method) of bulk graphite [17]. They are less effective for extensive scale producing. Chemical methods are a useful way to get bulk-scale graphene [18]. Yet, the synthesis of graphene has been focused fundamentally on chemical derivatization, intercalation, oxidation-reduction, thermal expansion, or through the use of surfactants [19-23]. The most well-known way to deal with graphite exfoliation is the use of strong oxidizing agents to form graphene oxide (GO) [22,23], which can be reduced to form reduced graphene oxide rGO. It can be readily dispersed in water to produce a large scale of graphitic films [23-27].

2. Experimental

2.1 Preparation of reduced graphene oxide (rGO)

Graphene oxide (GO) was prepared by modified Hummers-Hoffman's method [28]. 5 g of graphite powder was added to 120 ml of 98% of H_2SO_4 in an ice bath with continuous stirring and temperature didn't exceed 20°C. Then 2.5 g $NaNO_3$ followed by 20 g of $KMnO_4$ was added gradually to prevent a rapid increase in temperature. The mixture was stirred for 2 h in an ice bath and 1 h at 35°C. After that sample would be like a paste, then 250 ml of distilled (H_2O) was added drop by drop in an ice bath, which causes effervescence and temperature suddenly increased to 98°C then cooled after 10 min. Next, 50 ml of H_2O_2 was added, lead to convert sample into oily color. The mixture was heated at 90°C for 30 min, centrifuged and washed by

boiling distilled water until the product becomes neutral. The product was dried at 65°C for 24 h to get GO. Reduced grapheme oxide (rGO) was synthesized by chemical reduction of GO. This is done by dispersin 0.1 g of GO in 20 ml distilled water and ultrasonicated for 30 min to confirm dispersion, then 3 ml of hydrazine NH_2-$NH_2.H_2O$ was added to the solution. The mixture was stirred at 80°C for 1h. The product was washed and filtrated until it became neutral, then it kept one day at 80°C to get rGO.

2.2 Preparation of polyaniline (PANI)

PANI was synthesized by in-situ oxidation-polymerization [29]. In the typical procedures, Aniline monomer was prepared by dissolving 1.8 ml of aniline in 100 ml of 1M of HCl to form aniline hydrochloride. By using $(NH_4)_2S_2O_8$ as the oxidant, 100 ml of 0.1M was titrated drop by drop with continuous stirring for 3 h in an ice bath. The solution was kept for 24 h to complete polymerization, then washed with distilled water to remove the excess of oxidant and unreacted monomers. Finally, the resultant polymer was obtained after drying at 60°C for several hours until getting a constant weight of the sample.

2.3. Preparation of supercapacitors working electrodes

Electrodes were prepared by mixing based material of (rGO, PANI, and PANI mixed with rGO with mass ratio 1:1 rGO@PANI with carbon black and polyvinylidene fluoride (PVF) with percent ratio 75:15:10, respectively with few drops of ethanol to get slurry form, then it was spread on stainless steel (SS), then dried at 80°C for 1h to vaporize solvent and achieve the best adhesion on surface of substrate.

2.4. Characterizations and measurements

In the present study, all prepared samples were characterized by different techniques. X-ray diffraction (XRD) patterns were analyzed by using a Philips diffractometer PW 1710 with Cu-Kα irradiation (λ= 0.15418 nm) at diffraction angles of 2θ between 5° to 80° at a scan rate of 5° min⁻¹. Scan electron microscopy (SEM) was carried out by using JEOL-JSM-6510 LV. FT-IR spectra were performed by FT-IR spectrophotometer model Thermo Scientific Nicolet using KBr pellet technique in the range of 4000-400 cm⁻¹.

Electrochemical measurements of the prepared electrodes used to evaluate the capacitive parameters of the investigated materials. Cyclic voltammetry (CV) was used to calculate the specific capacitance of prepared samples depending upon the integrated area method. The galvanostatic charge-discharge technique (GCD) was used to calculate specific capacitance depending upon the discharge time. Electrochemical impedance spectroscopy (EIS) was used to detect prepared materials resistance. The electrochemical measurements were carried out using a triple system in which the prepared samples used as working electrodes vs. saturated calomel electrode as (SCE) a reference electrode, while Pt electrode (Pt.E) used as a counter electrode in 6M KOH aqueous electrolyte. Capacitance was measured by CV and GCD method by

using (Digi-Ivy 2116 B), the USA, in which the prepared materials were filmed on SS, CV was performed between -1.5:0.5 V at scan rate 5 mV/s and measured at current density (I_d) 500 mA/g. EIS was measured with (Metrohm auto lab PGSTAT 204). Netherlands. The prepared materials were filmed on SS and measured at current ranged from 10 μA:100 mA, frequency ranged from 0.1 Hz:100 kHz and fixed potential 10 mV.

3. Results and discussions

3.1 Chemical characterizations

Fig. 1 shows the XRD pattern of reduced graphene oxide (rGO) and graphene oxide (GO) to give information on the reduction degree of GO. The XRD pattern of GO shows two peaks at 2θ = 10.09° and 2θ = 42 characterized for graphene oxide peaks of (001) and (004) plans [30], respectively. These peaks are disappeared in XRD of G with an appearance of a new peaks at 2θ = 26.5° corresponding to (002) graphene plane. This refers to that GO is almost converted into graphene indicating the effective reduction process. The crystallite size of rGO was estimated using Scherrer's equation and found to be 3 nm.
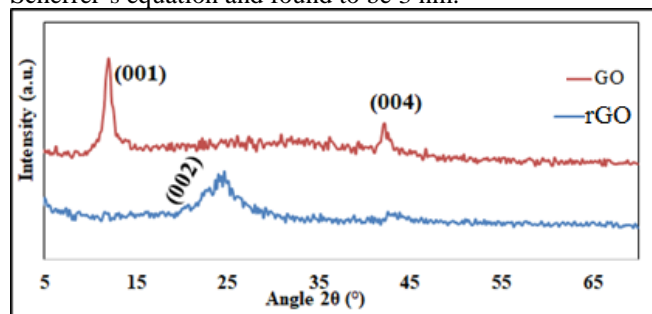
Fig (1): XRD patterns of rGO, and rGO

The XRD pattern of PANI given in Fig. 2 shows main diffraction peaks with amorphous nature at about 2θ = 21° and 25° corresponding to the periodicity parallel and perpendicular to PANI chains, respectively [31].
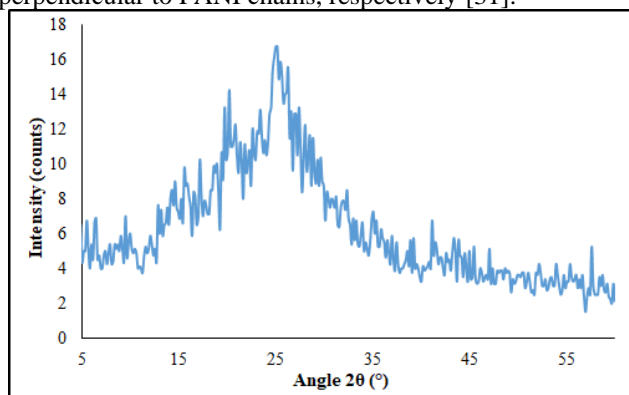
Fig (2): XRD pattern of PANI

Fig. 3 shows FT-IR of GO and rGO samples. Several types of oxygen functionalities in both samples was confirmed by the presence of many bands. It showed the presence of broadband at 3400 cm⁻¹ that can be attributed to the O-H stretching vibrations of the C-OH groups and water [32, 33]. It is also showed bands at 1640 cm⁻¹ (stretching

vibrations from C=C), at 1650 cm^{-1} (skeletal vibrations from unoxidized graphitic domains) [34, 35], and at 1050 cm^{-1} (C-O stretching vibrations). However, stretching vibrations from C=O at 1740 cm^{-1} were still observed and C-O stretching vibrations at 1050 cm^{-1} turn out to be sharper, which were caused by remaining carboxyl groups even after hydrazine reduction [36].
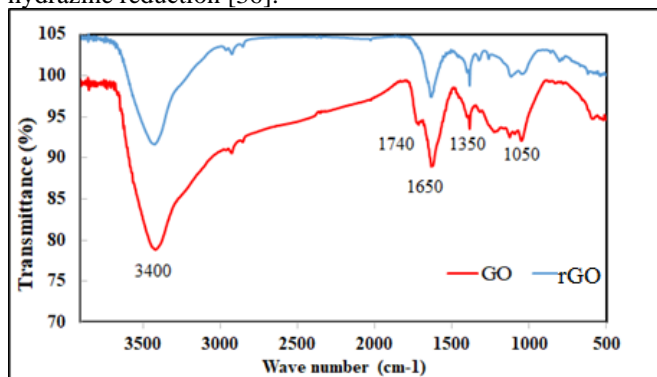
Fig (3): FT-IR pattern of G, and rGO

Fig. 4 shows the FT-IR spectrum of PANI. It shows C-H aromatic group at 2900 cm^{-1}, C=N at 1566 cm^{-1}, C=C at 1490 cm^{-1}, C-N at 1290 cm^{-1}, and bending of the quinoid ring (C=N) at 1105 cm^{-1}. The polymerization of aniline can be approved by the existence of spectral peaks at 1490 and 1566 cm^{-1} owing to stretching of the benzenoid and quinoid rings, respectively, for the acid doped PANI. These

outcomes refer to that pure PANI is already doped and is present in conducting emeraldine salt form [37]. The peak at 1290 cm^{-1} matching to C-N stretching of secondary amine in the main polymer chain.
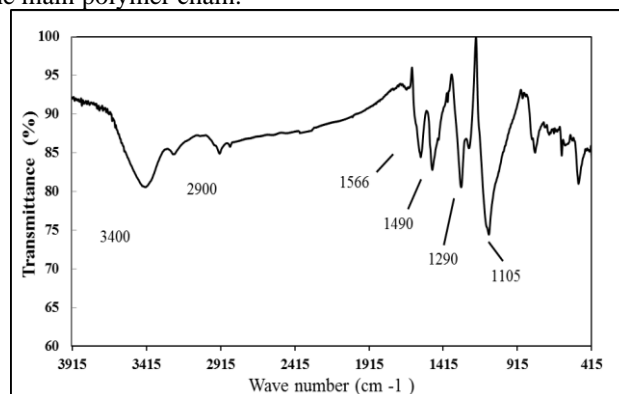
Fig (4): FT-IR pattern of PANI

Surface morphology of G shows the hexagonal nanolayer formation of rGO, which found stacked on each other. Well-defined structure and diffraction confirm the crystalline structure of rGO, which observed in Fig. 5 (a).

SEM images of PANI shows that prepared material was amorphous clusters of the granular morphology of PANI with average grain size 0.4 μm, which shown in Fig. 5 (b).
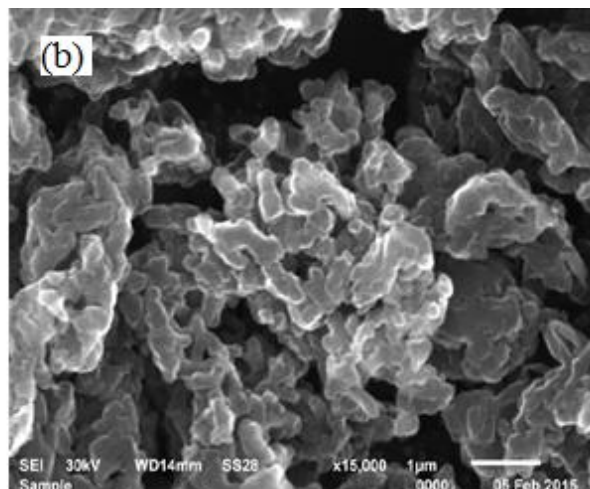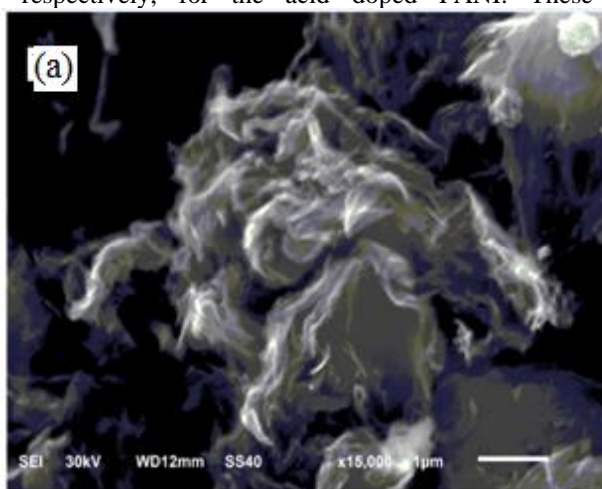
Fig (5): SEM images of (a) rGO nanosheets, (b) PANI

3.2. Electrochemical measurements

The results of CV measurements of PANI and rGO-PANI composite samples on SS in 6 M aqueous KOH solution at a scan rate of 5 mV/s are represented in Fig. 6. rGO curve showed a semi-rectangular shape without any formation of redox peaks. This agrees with the electric double layer capacitance found in carbon-based materials. The CV of PANI and rGO@PANI curves showed the same behavior,

where two pairs of redox peaks demonstrating reversible charge-discharge behavior are observed at -1.2 V, and -0.9 V. This can be ascribed to the redox transition of PANI between a semiconducting state (leucoemeraldine salt) and a conducting state (polaronic emeraldine form) The pair of peaks at around -0.85 V, and -0.9 V can be originated from the emeraldine–pernigraniline transformation [38-40].
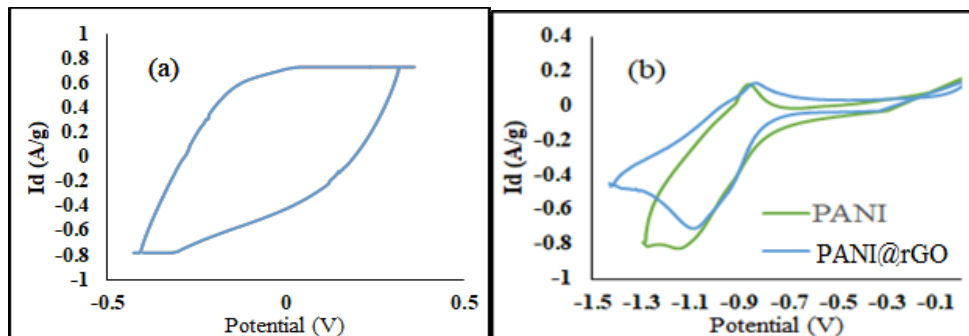
Fig (6): CV of (a) rGO, (b) PANI, and rGO@ PANI

The two pairs of redox peaks observed in CV curve of rGO@PANI composite, which is similar to that of PANI indicates that the capacitance of rGO@ PANI nanocomposite come mainly from the pseudocapacitance of PANI besides the double layer of rGO. The redox peaks are slightly decreased in rGO@ PANI than that in PANI due to decreasing the effect of rGO on the pseudocapacitive mechanism of PANI.

The specific capacitance (C_{sp}) was calculated from CV data according to equation (1) [40] and the data obtained are listed in Table (1)

$$C_{sp} = \frac{2}{\Delta V.v.m} \int_{-V}^{+V} I(V) \, dV \qquad (1)$$

Where (C_{sp}) is specific capacitance (F/g), (V) is applied potential (V), (v) is potential scan rate (V/s), (I) is current (A), and (m) is mass of active material of electrode (g).

The charge-discharge curves of the investigated samples are represented in Fig. 7. It shows a negative exponential slope with varied internal resistance (IR) drop at discharge current I_d of 500 mA/g, indicating good capacitive behaviors for the prepared electrodes. Low (IR) is important in energy storage devices, where less energy is consumed to generate heat during charge-discharge processes. The longest discharge time of electrode indicates the highest capacitance and best electrochemical performance. C_{sp} values were calculated by the following equation (2) [40].

$$C_{sp} = \frac{I\Delta t}{m \, \Delta V} \qquad (2)$$

Where (C_{sp}) is specific capacitance (F/g), (I) is discharge current (A), (ΔV) is discharged potential (V), (Δt) is discharge time (sec), and (m) is mass of active material of electrode (g). The results obtained are listed in Table 1.
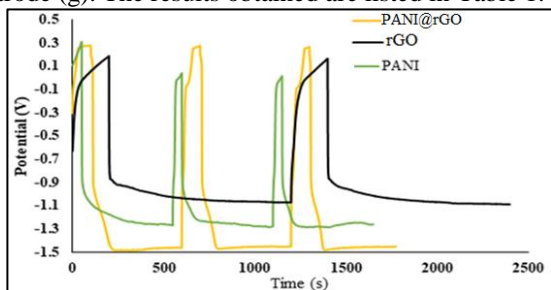
Fig (7): Galvanostatic charge-discharge GCD of prepared electrodes

Electrochemical stability is one of device quality and practical application. In order to evaluate charge storage capacity, the durability of a cycle lifetime and various electrical parameter, the GCD analysis of supercapacitor assemblies was performed at a current density of 325 mA/g on both substrates for 250 charge-discharge cycles. Charge-discharge curves show reversible characteristics between 1st, and 250th, which implies to electrode stability and capacitance efficiency for each electrode at Fig. 8, and results are shown in Table 1.

Electrode efficiency (E_{eff} %) was calculated from equation (3) [41]:

$$E_{eff} = (C_n / C_1) \times 100 \qquad (3)$$

In which (C_n) is the capacitance of electrode of nth cycles, (F/g) (C_1) is the capacitance of the 1st cycle (F/g).

The energy density (E_d), and Power density ((P_d) are two important parameters in evaluating the electrochemical performance of the electrode materials and the supercapacitors. The two parameters (E_d, Wh/kg), and (P_d, W/kg) were calculated using the following equations [40, 41]:

$$E_d = \frac{1}{2} C_{sp} \, \Delta V^2 \qquad (4)$$

$$P_d = \frac{E}{t} \qquad (5)$$

In which C_{sp} is the specific capacitance of the supercapacitor (F/g), ΔV is the voltage change during the discharge process after IR drop in (V), and t is the time for a sweep segment (h). The results obtained are listed in Table 1.
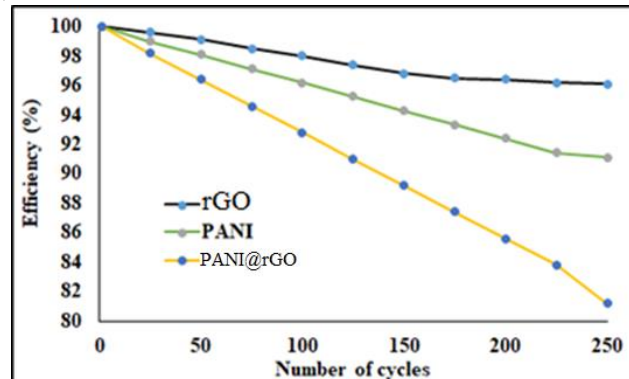
Fig (8): Electrochemical stability of prepared electrodes

Table (1): Electrochemical parameters of prepared electrodes

Sample	C_{sp} (F/g)	E (W/kg)	P (W/kg)	Efficiency after 100 cycles (%)	R_S (Ω)	R_{ct} (Ω)
PANI	18 (37.2)	9.2	50	92.1	2	498
rGO	60 (70.5)	15.6	182.5	97.1	1.6	5
rGO@PANI	16 (22.3)	6.5	153	81.2	5	7000

(C_{sp}) is C_{sp} from GCD

The impedance spectra of the investigated materials are represented as Nyquist plots in Fig. 9. EIS showed a semicircle in the high-frequency section and a linear part in the low-frequency region [42,43]. The diameter of the semicircle associates with the interfacial charge-transfer resistance, which frequently descriptions for the resistance of the electrochemical response on the electrode (Faradaic resistance). rGO shows high electronic diffusion and conductivity with lower charge transfer resistance.

Because the same electrolyte was employed in all EIS measurements, the obtained data refer to that the internal resistance and/or the contact resistance of rGO are less than those of PANI film and rGO@PANI nanocomposite. The EIS data in the low-frequency section essentially links to the amount of Warburg resistance, which displays the diffusion of redox species in the electrolyte, and a sharper plot normally points to faster ion diffusion. The slope line of PANI is greater than that of rGO@PANI film, implying the excessive porosity of the polymer. rGO - framework can certainly hinder speedier ion diffusion. Collectively, these electrochemical characterizations corroborative reveal that the rGO@PANI nanocomposite acquires worse capacitive properties than PANI or rGO, due to formation emeraldiene base, which has low specific capacitance and poor conductivity. EIS is shown in Fig. 9, and results of R_S and R_{CT} of all material were summarized in Table 1.
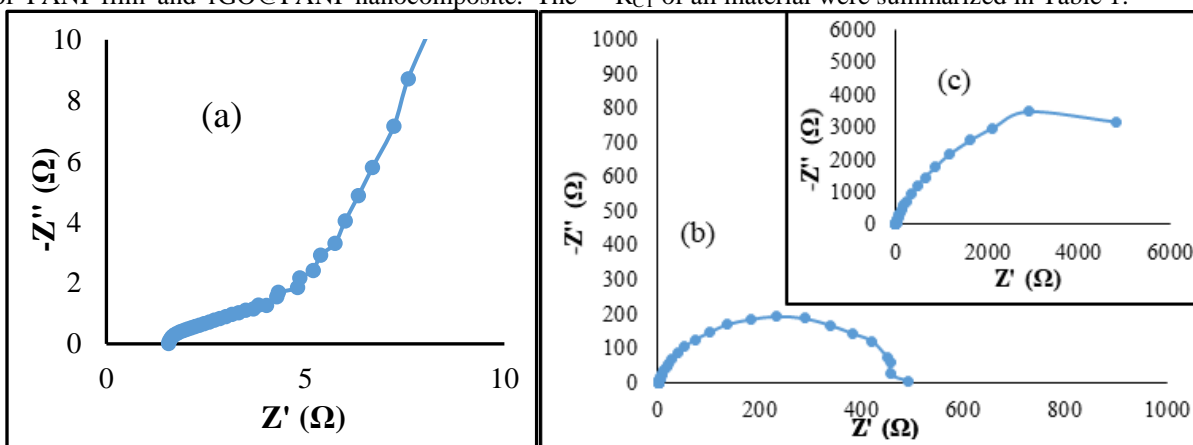
Fig (9): EIS of (a) rGO, (b) PANI, and (c) rGO@PANI

4. Conclusions

In conclusion, polyaniline was synthesized by chemical polymerization. rGO was prepared by a modified Hummers' method followed by chemical reduction. Both of the prepared materials were investigated to assure the exact preparation by XRD and FT-IR and SEM. The electrochemical performance was studied by using CV, GCD, and EIS curves. The electrochemical analysis showed the pseudocapacitive behavior of PANI while rGO shows electric double layer behavior. The PANI@rGO composite prepared by grinding PANI@rGO shows pseudocapacitive behavior also, but with low capacitance in compare with PANI or G separately, due to charge opposing collision and formation of emeraldine base which has lower capacitance.

References

[1] A. B. Moghaddam, T. Nazari, "Preparation of polyaniline/nanometer-scale alumina composite by the potential cycling method", Int. J. Electrochem. Sci., 3 (2008) 768-776

[2] A. S. Sarac, M. Ates, and B. Kilic, "Electrochemical impedance spectroscopic study of polyaniline on platinum, glassy carbon and carbon fiber microelectrodes", Int. J. Electrochem. Sci., 3 (2008) 777-786.

[3] N. Ahmad, and A. G. MacDiarmid, "Inhibition of corrosion of steels with the exploitation of conducting polymers", Synth.Met., 78 (1996) 103-110.

[4] S. Kuwabata, S. Masui, and H. Yoneyama, "Charge-discharge properties of composites of $LiMn_2O_4$ and polypyrrole as positive electrode materials for 4 V class of rechargeable Li batteries", Electrochim. Acta, 44 (1999) 4593- 4600.

[5] T. L.Rose, S. D. Antonio, M. H. Jillson, A. B. Kron, R. Suresh, and F. Wang, "A microwave shutter using conductive polymers", Synth. Met., 85 (1997) 1439-1440.

[6] T. Makel, S. Pienimaa, T. Taka, S. Jussila, and H. Isotalo, "Thin polyaniline films in EMI shielding", Synth. Met., 85 (1997) 1335-1336.

[7] R. Mathur, D. R. Sharma, S. R. Vadera, and N. Kumar, "Doping of emeraldine base with the monovalent bridging iron oxalate ions and their transformation into nanostructured conducting polymer composites", Acta mater., 49 (2001) 181–187.

[8] L. Li, H. Liu, Y. Wang, J. Jiang, and F. Xu, "Preparation and magnetic properties of Zn- Cu- Cr- La ferrite and its nanocomposites with polyaniline", Colloid Interface Sci., 321 (2008) 265–271.

[9] A. G. MacDiarmid, and A. J. Epstein, "Secondary doping in polyaniline" Synth. Met., 69 (1995) 85-92.

[10] J. C. Aphesteguy, and S. E. Jacobo, "Composite of polyaniline containing iron oxides", Physica B, 354 (2004) 224–227.

[11] S. E. Jacobo, J. C. Aphesteguy, R. L. Anton, N.N. Schegoleva, and G.V. Kurlyandskaya, "Influence of the preparation procedure on the properties of polyaniline-based magnetic composites", Eur. Polym. J., 43 (2007) 1333–1346.

[12] Y.I. Kim, Don Kim, C. Lee, "Synthesis and characterization of $CoFe_2O_4$ magnetic nanoparticles prepared by temperature-controlled coprecipitation method", Physica B, 337 (2003) 42–51.

[13] R. Kiebooms, R. Menon, and K. H. Lee, in "Handbook of advanced materials for electronics and photonics", (H. S. Nalwa, Ed.), 8, Academic Press, San Diego, (2001).

[14] C. N. R. Rao, and A. K. Sood, "Graphene: Synthesis, properties, and phenomena", Wiley-VCH Verlag GmbH & Co. KgaA, (2013).

[15] C. Berger, Z. Song, X. Li, et al. "Electronic confinement and coherence in patterned epitaxial graphene", Science, 312 (2006) 1191–1196.

[16] R. Ruoff, "Graphene: Calling all chemists.", Nat. Nanotechnol., 3 (2008) 10–11.

[17] S. Chakraborty, W. Guo, R. H. Hauge, and W. E. Billups, "Reductive alkylation of fluorinated graphite", Chem. Mater., 20 (2008) 3134–3136.

[18] N. Behabtu, J. R. Lomeda, M. J. Green, et al. "Spontaneous high-concentration dispersions and liquid crystals of graphene", Nat. Nanotechnol., 5 (2010) 406–411.

[19] J. R. Lomeda, C. D. Doyle, D. V. Kosynkin, W. F. Hwang, and J. M. Tour "Diazonium functionalization of surfactant-wrapped chemically converted graphene sheets". J. Am. Chem. Soc, 130 (2008) 16201–16206.

[20] A. L. Higginbotham, J. R. Lomeda, A. B. Morgan, and J. M. Tour, "Graphite oxide flame-retardant Polymer

nanocomposites", J. Appl. Mater. Interfaces, 1 (2009) 2256–2261.

[21] D. R. Dreyer, S. Park, C. W. Bielawski, and R. Ruoff, "The chemistry of graphene oxide", J. Chem. Soc., 39 (2010) 228–240.

[22] F. Uhl, C. Wilkie, "Preparation of nanocomposites from styrene and modified graphite oxides", Polym. Degrad. Stab, 84 (2004) 215–226.

[23] S. Stankovich, R. Piner, X. Chen, N. Wu, S. Nguyen, and R. Ruoff, "Stable aqueous dispersions of graphitic nanoplatelets via the reduction of exfoliated graphite oxide in the presence of poly(sodium 4-styrenesulfonate)", J. Chem. Mater., 16 (2006) 155–158.

[24] T. Ishikawa, T. Nagaoki, and S. Kogyo "New carbon industry", 2nd ed., 125-36, Kindai hensyusya, Tokyo, (1986).

[25] P. Touzain, R. Yazumi, and J. Maire "Insertion compounds of graphite with improved performances and electrochemical applications of those compounds". U.S. Patent 4584252, April 22, 1986.

[26] I. Barsukov, C. Johnson, J. Doninger, and V. Barsukov,"New carbon-based materials for electrochemical and fuel cells energy storage systems: Batteries, supercapacitors", Springer in cooperation with NATO Public Diplomacy Division, 229, (2006).

[27] M. Inagaki, H. Konno, and O. Tanaike, "Carbon materials for Electrochemical Capacitors", J. Power Sources, 195 (2010) 7880–7903.

[28] E. L. Guerra, A. N. Shanmugharaj, W. S. Choi, and S. H. Ryu, "Thermally reduced graphene oxide-supported nickel catalyst for hydrogen production by propane steam reforming", Appl. Catal., A, 468 (2013) 467-474.

[29] Z. Durmus, A. Baykal, H. Kavas, H. Sözeri, "Preparation and characterization of polyaniline (PANI)-Mn_3O_4 nanocomposite", Physica B, 406 (2011) 1114-1120.

[30] P. Ramesh, S. Bhagyalakshmi, and S. Sampath, "Preparation and physicochemical and electrochemical characterization of exfoliated graphite oxide. "J. Colloid Interface Sci., 274 (2004) 95–102.

[31] T. Abdiryim, Z. Xiao-Gang, and R. Jamal, "Comparative studies of solid-state synthesized polyaniline doped with inorganic acids", Mater. Chem. Phys., 90 (2005) 367–372.

[32] N. Padmavathy, and R. Vijayaraghavan, "Enhanced bioactivity of ZnO nanoparticles - an antimicrobial study", Sci. Technol. Adv. Mat., 9 (2008) 35004-35010.

[33] T. Zhang, D. Zhang, and M. Shen, "Low-cost method for preliminary separation of reduced graphene oxide nanosheets", Mater Lett., 63 (2009) 2051–2054.

[34] Si Y, and E. Samulski, "Synthesis of water-soluble graphene", Nano Lett., 8 (2008) 1679-1682.

[35] Y. Xu, H. Bai, G. Lu, C. Li and G. Shi, "Flexible graphene films via the filtration of water-soluble noncovalent functionalized graphene sheets", J. Am. Chem. Soc., 130 (2008) 5856–5857.

[36] D. Li, M. Müller, S. Gilje, R. Kaner, and G. Wallace, "Processable aqueous dispersions of graphene nanosheets", Nature Nanotechnol., 3 (2008) 101-105.

[37] J. Jiang, L. Liangchao, and X. Feng, "Polyaniline–LiNi ferrite core-shell composite: Preparation, characterization and properties", Mater. Sci. Eng. A, 456 (2007) 300-304.

[38] K. Zhang, L. Zhang, X. S. Zhao and J. Wu, "Graphene/polyaniline nanofiber composites as supercapacitor electrodes", Chem. Mater., 22 (2010) 1392–1401.

[39] J. J. Xu, K. Wang, S. Z. Zu, B. H. Han, and Z. X. Wei, " Hierarchical nanocomposites of polyaniline nanowire arrays on graphene oxide sheets with synergistic effect for energy storage", ACS Nano, 4 (2010) 5019-5026.

[40] T. Lee, T. Yun, B. Park, B. Sharma, H. K. Song, and B. S. Kim, " Hybrid multilayer thin film supercapacitor of graphene nanosheets with polyaniline: the importance of establishing intimate electronic contact through nanoscale blending", J. Mater. Chem., 22 (2012) 21092-21099.

[41] S. Mallika, and R. S. Kumar, "Review on ultracapacitor- battery", Int. J. Eng. Tech, 3 (2011) 37-43.

[42] B. Lee, and J. R. Yoon, "Preparation and characteristics of $Li_4Ti_5O_{12}$ with various dopants as an anode electrode for hybrid supercapacitor", Curr. Appl. Phys., 13 (2013) 1350-1353.

[43] E. L. Guerra, A. N. Shanmugharaj, W. S. Choi, and S. H. Ryu, "Thermally reduced graphene oxide-supported nickel catalyst for hydrogen production by propane steam reforming", Appl. Catal., A, 468 (2013) 467-474.